Quaternary Science Reviews 307 (2023) 108054

Contents lists available at ScienceDirect

Quaternary Science Reviews

journal homepage: www.elsevier.com/locate/quascirev

Distal tephra reveal new MIS 5e Kos eruptions: Implications for the chronology and volcanic evolution histories in the Eastern Mediterranean region

Shuang Zhang [a, *], Simon Blockley [a], Simon J. Armitage [a, b], Chris Satow [a], Christina Manning [c], Omry Barzilai [d, e], Elisabetta Boaretto [e], Dustin White [f], Rhys Timms [g]

[a] Department of Geography, Royal Holloway University of London, Egham, Surrey, TW20 0EX, UK
[b] SFF Centre for Early Sapiens Behaviour (SapienCE), University of Bergen, Bergen, Norway
[c] Department of Earth Sciences, Royal Holloway University of London, Egham, Surrey, TW20 0EX, UK
[d] Archaeological Research Department, Israel Antiquities Authority, POB 586, 91004, Jerusalem, Israel
[e] Max Planck-Weizmann Center for Integrative Archaeology and Anthropology, DANGOOR Research Accelerator Mass Spectrometry Laboratory, Weizmann Institute of Science, 7610001, Rehovot, Israel
[f] Department of Chemistry, University of York, York, UK
[g] School of Archaeology, Geography and Environmental Science, University of Reading, Reading, RG6 6AB, UK

ARTICLE INFO

Article history:
Received 21 November 2022
Received in revised form
12 March 2023
Accepted 18 March 2023
Available online 30 March 2023

Handling Editor: Giovanni Zanchetta

Keywords:
Kos-nisyros-yali volcanic complex
Kos plateau tuff
Trace elements
Cryptotephra
Tephrochronology
Tephrostratigraphy
Eastern mediterranean
MIS 5e

ABSTRACT

The Kos Plateau Tuff (KPT), was an enormous caldera forming eruption originating from a vent within the Kos/Nisyros/Yali volcanic complex, occurring at 161 ka. It is the largest recognised Late Quaternary eruption in the Eastern Mediterranean. With its distinctive, highly silicic chemical composition, the resulting ash deposits have been used both as a synchronous marker for palaeoenvironmental records in the region, and to provide information on eruption processes and magnitude. Here, we describe ash layers detected at multiple sites (deep-sea sequences and a terrestrial archaeological site) with ages generated by radiometric dating and sapropel correlation, to demonstrate the existence of a later, but geochemically similar eruption from the Kos volcano which has not previously been identified in proximal volcanic units. This eruption is dated to MIS 5e (~124–129 ka), i.e. ~40 kyr younger than the KPT. This tephra marks the start of MIS5e, and presents a rare opportunity to independently and precisely align paleoenvironmental records and archaeological sites during a time of rapid warming and sea level rise analogous to the present day. The presence of multiple tephras also implies the possibility of multiple eruptions during this period. This adds to our knowledge of the active and hazardous nature of Kos/Nisyros/Yali volcanic complex.

1. Introduction

The Kos-Nisyros-Yali volcanic field is located in the eastern Aegean Volcanic Arc (Fig. 1). It has produced numerous volcanic eruptions over the last 3 Myr (Bachmann et al., 2019). The Kos-Nisyros-Yali volcanic complex is of great research importance, as it sits in a densely populated area and has produced multiple explosive volcanic eruptions during the late Quaternary. The Kos Plateau Tuff (KPT) is recognised as the largest upper Pleistocene eruption in the Aegean Arc (Bachmann et al., 2019), depositing pyroclastic material which travelled over 60 km across the sea surface from the vent and visible ash layers in Black Sea sediments (Allen et al., 1999; Wegwerth et al., 2019). The KPT is a key regional tephra that allowed the study of magma-water interaction, transportation of pyroclastic flows, and conduit flow processes (Allen, 2001; Dufek and Bergantz, 2007; Bouvet de Maisonneuve et al., 2009). It is seen as the only Kos eruption forming the end of a highly silicic shallow phase of volcanism in the volcanic field, followed by a less explosive mafic period before a rhyolitic eruption from Nisyros (Bachmann et al., 2019).

The KPT is in many Eastern Mediterranean marine sequences and is a significant tephra marker (labelled the W-3; Vinci, 1985), underpinning many regional chronologies. Dating by K–Ar/Ar–Ar

* Corresponding author.
E-mail address: shuang.zhang.2017@live.rhul.ac.uk (S. Zhang).

https://doi.org/10.1016/j.quascirev.2023.108054

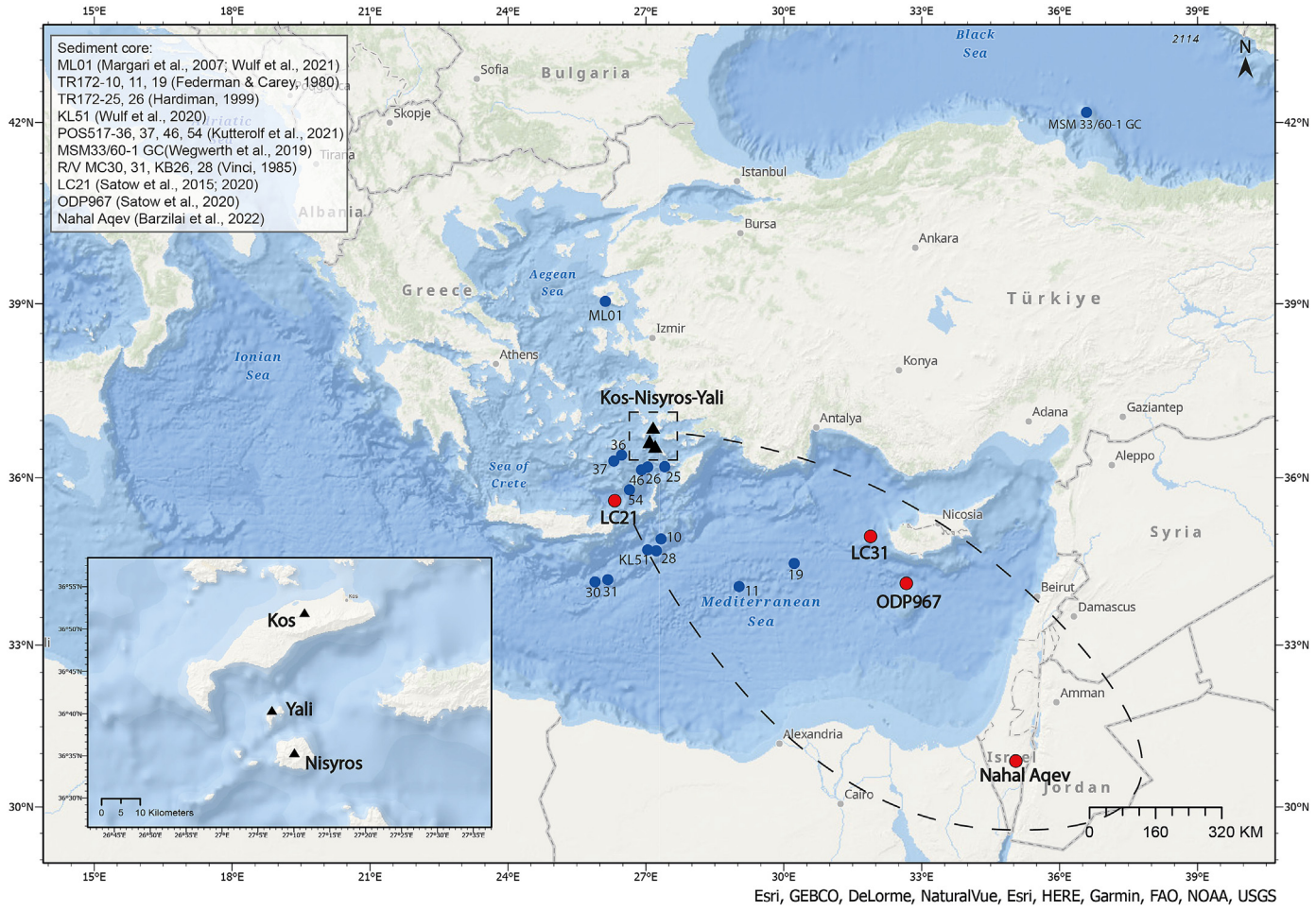

Fig. 1. Map of the Kos-Nisyros-Yali volcanic field (inset) and sites containing the MIS 5e Kos tephra (red dots; Barzilai et al., 2022; Satow, 2012) or KPT (blue dots; Federman and Carey, 1980; Hardiman, 1999; Kutterolf et al., 2021; Margari et al., 2007; Satow et al., 2015; Vinci, 1985; Wegwerth et al., 2019; Wulf et al., 2020, 2021). The dashed line indicates an estimated dispersal range for the MIS 5e Kos tephra.

on sanidine and Pb–U in zircons consistently provides an age of ~161 ± 1 ka for this eruption (Smith et al., 1996, 2000; Bachmann et al., 2010a; Guillong et al., 2014). However, recent studies have reported tephra layers dated to MIS5e with KPT-like compositions (Satow et al., 2015, 2020; Barzilai et al., 2022). Products of the Milos and Acigöl volcanic complexes in central Anatolia also have similar major element compositions to the KPT, and are only distinguishable by trace element analysis (Kutterolf et al., 2021; Tomlinson et al., 2015). This means that the KPT is not an unambiguous isochron in the region.

We present major and trace element analyses of several highly evolved rhyolitic tephra layers from the MIS 5e levels of three marine cores (LC21, ODP967 and LC31) and an archaeological site in Isreal (Nahal Aqev). We compare them to the major and trace element signatures of known eruptions from the Kos, Milos and Acigöl volcanic centres, to demonstrate the existence of previously unknown volcanic eruption(s) from Kos.

2. Methods

Marine core LC31 was recovered during R.V. Marion Dufresne Cruise 81 (1995) and is located at 34° 59.76′ N and 31° 09.81′ E, west-northwest of Cyprus (2300 m water depth; Fig. 1). In LC31, two luminescence dating samples were taken approximately 10 cm above and below the visible tephra at 6.37 m composite depth (LC31 6.37), proving an age of 129.6 ± 6 ka (see Supplementary text). This visible tephra was treated with 10% HCl solution, sieved to 15–125 μm, extracted at a density of 2.0–2.55 g/cm^3 and bulk mounted on epoxy stubs (Blockley et al., 2005). Major element compositions were determined by WDS-EPMA, and trace elements by LA-ICP-MS (see Supplementary information) and compared with previously published rhyolitic tephra with Kos-like major element compositions from marine cores ODP967 (Satow, 2012; Satow et al., 2020), LC21 (Satow et al., 2015, 2020) and archaeological excavation at Nahal Aqev, Isreal (Barzilai et al., 2022). As these samples have been analysed using different instruments with different analytical setups (see Supplementary), the level of data comparability is addressed by calculating the average of 2 standard deviations of secondary standards (Fig. 3). Although these tephras have been analysed with different glass standards, (Atho-G and Lipari), the compositions of these two standards were similar to each other and also to these tephras, all are highly silicic suitable for comparing the precision of data (see Supplementary).

3. Results and discussion

3.1. Tephrostratigraphy of the sequences containing MIS 5e tephra

Four sites with tephra and cryptotephra layers with major element profiles similar to Kos, Milos or Acıgöl are examined in this

study: marine cores ODP967, MD81-LC21, MD81-LC31 and one terrestrial archaeological site Nahal Aqev (NAQ) in the Negev Desert (Fig. 1). ODP967 contains two crypto and one visible tephra layers with Kos-like major element composition (ODP967 7.610, 8.460, 8.870; Satow, 2012). ODP967 8.870 is a visible layer correlated to KPT. ODP967 8.460 is a small cryptotephra layer with only 42 shards per gram, potentially represents remobilisation of ODP 8.870. ODP967 7.610 occurs in sapropel 5, with over 2500 shards/g. Each ODP967 tephra occurs as a discrete peak with no background tephra signal in surrounding material. LC21 has one cryptotephra layer (LC21 993.5) in sapropel 5 with 42,610 shards/g, another cryptotephra layer (LC21 10.345) sitting 50 cm below it with 2357 shards/g, and a visible layer (LC21 12.465, correlated to KPT) at the base of the sequence. LC21 993.5 and LC21 10.345 both immediately predate MIS 5e (Satow et al., 2015, 2020). The LC21 stratigraphy shows no evidence for reworking and there are no shards in the 50 cm sediment in between the two tephra units. The NAQ tephra is an abundant cryptotephra layer with 21,433 shards/g. LC31 contains one 8-cm thick visible tephra at 6.37 m composite depth with a Kos-like signal.

3.2. Geochemical analyses

The major element compositions of MIS 5e tephra layers (ODP967 7.610, ODP967 7.460, LC21 993.5, LC21 10.345 and NAQ) are provided in previous publications (Satow, 2012; Satow et al., 2015, 2020; Barzilai et al., 2022). Their major and trace element compositions are mostly overlapping from those of LC31 6.37 (Fig. 3a–d; Table 2). However, LC31 6.37 and the NAQ tephra sit at the low and high ends of the compositional array observed on the TAS diagram (Fig. 3b), where LC31 6.37 shows a lower SiO_2 and higher total alkali content compared to the NAQ tephra showing the higher SiO_2 and lower total alkali contents. It can be seen that LC21 993.5 shows a large compositional range with total alkali between 7.0 and 8.9% (Fig. 3b; Table 1), across the compositional ranges of both LC31 6.37 and NAQ tephra. However, the total number of LC21 993.5 shards analysed is low due to their low concentration in the sediment (Satow, 2012). This observation also applies to LC21 10.345, ODP967 7.610 and ODP967 8.460 (Satow, 2012; Satow et al., 2015). As the precision and accuracy of glass standards are good (see Supplementary), this degree of compositional variability on a small number of shards almost certainly means the actual variation is greater. Under sampling almost always leads to an under estimation of the heterogeneity of the sample. This might imply a bigger compositional range of this group of tephra, which covers the both ends of compositional ranges of LC31 6.37 and NAQ tephra but needs chemical acquisition on larger number of shards in further studies. It remains challenging that all these tephras were analysed using different instrumental setups with different beam sizes. Once the analytical uncertainty has been considered it

Table 1
A summary of averaged major elements compositions of the MIS 5e group of tephras (this study; Satow, 2012; Satow et al., 2015, 2020; Barzilai et al., 2022), distal and proximal KPT (Satow, 2012; Satow et al., 2015; Wulf et al., 2020; Kutterolf et al., 2021), Milos (Kutterolf et al., 2021) and Acıgöl (Tomlinson et al., 2015). Full geochemical data sets acquired in this study are available in the Supplementary material file.

Name	SiO2	TiO2	Al2O3	FeO	MnO	MgO	CaO	Na2O	K2O	P2O5	Volcano	Reference
Nahal Aqev	78.27	0.08	12.32	0.51	0.06	0.06	0.59	4.29	3.82	0.01	Kos	Barzilai et al., 2022
2s.d.	0.84	0.01	0.59	0.13	0.01	0.00	0.08	1.09	1.56	0.03		
ODP967 7.61	77.63	0.09	12.73	0.51	0.05	0.07	0.57	3.61	4.74	0.02	Kos	Satow et al. (2020)
2s.d.	0.43	0.06	0.17	0.14	0.08	0.05	0.06	0.57	0.52	0.04		
ODP967 8.46	77.62	0.09	12.76	0.40	0.06	0.05	0.52	3.88	4.61	N/A	Kos	Satow (2012)
2s.d.	0.07	0.03	0.31	0.04	0.07	0.02	0.05	0.54	0.24			
ODP967 8.87	78.27	0.09	12.35	0.52	0.04	0.06	0.57	3.60	4.51	N/A	Kos	Satow (2012)
2s.d.	0.43	0.05	0.20	0.14	0.07	0.04	0.09	0.41	0.48			
LC21 993.5	77.67	0.08	12.64	0.54	0.06	0.07	0.57	3.38	4.99	N/A	Kos	Satow et al. (2020)
2s.d.	0.94	0.07	0.45	0.17	0.08	0.04	0.06	1.06	0.32			
LC21 10.345	77.76	0.08	12.67	0.50	0.07	0.04	0.56	3.44	4.87	N/A	Kos	Satow et al. (2015)
2s.d.	0.83	0.04	0.22	0.11	0.10	0.03	0.05	1.02	0.46			
LC21 KPT	78.03	0.08	12.19	0.55	0.06	0.06	0.57	3.71	4.74	N/A	Kos	Satow et al. (2015)
2s.d.	0.51	0.05	0.31	0.12	0.09	0.03	0.07	0.48	0.45			
KPT-frothy	77.51	0.08	12.65	0.53	0.06	0.05	0.59	3.80	4.72	0.01	Kos	Kutterolf et al. (2021)
2s.d.	0.64	0.03	0.36	0.11	0.07	0.03	0.04	0.25	0.11	0.02		
KPT-qu-rich	77.51	0.08	12.70	0.58	0.07	0.06	0.58	3.69	4.71	0.02	Kos	Kutterolf et al. (2021)
2s.d.	0.48	0.04	0.35	0.11	0.10	0.04	0.02	0.50	0.25	0.03		
KL51-510	78.09	0.07	12.88	0.51	0.05	0.06	0.54	3.15	4.62	0.03	Kos	Wulf et al. (2020)
2s.d.	0.78	0.05	0.22	0.17	0.06	0.02	0.05	0.38	0.50	0.05		
LC31 6.37	77.09	0.08	12.95	0.52	0.06	0.06	0.58	3.82	4.83	0.01	Kos	This study
2s.d.	0.57	0.01	0.58	0.14	0.01	0.03	0.06	0.36	0.29	0.01		
KPT (POS cores)	77.60	0.10	12.68	0.58	0.06	0.05	0.62	3.67	4.64	0.01	Kos	Kutterolf et al. (2021)
2s.d.	0.62	0.04	0.34	0.13	0.08	0.05	0.08	0.40	0.56	0.03		
Guneydag	77.58	0.03	12.73	0.69	0.07	0.01	0.40	4.00	4.38	0.01	Acigöl	Tomlinson et al. (2015)
2s.d.	1.01	0.03	0.66	0.16	0.06	0.02	0.09	0.53	0.32	0.02		
Korudag	77.33	0.03	12.76	0.77	0.07	0.02	0.42	4.11	4.40	0.01	Acigöl	Tomlinson et al. (2015)
2s.d.	0.80	0.04	0.40	0.16	0.06	0.03	0.18	0.12	0.10	0.02		
Milos S1	78.06	0.10	12.69	0.72	0.06	0.12	0.91	3.92	3.40	0.02	Milos	Kutterolf et al. (2021)
2s.d.	0.38	0.04	0.25	0.14	0.08	0.05	0.04	0.35	0.10	0.03		
Milos S2	78.08	0.11	12.63	0.73	0.06	0.11	0.89	3.88	3.48	0.02	Milos	Kutterolf et al. (2021)
2s.d.	0.59	0.06	0.32	0.16	0.06	0.05	0.09	0.40	0.15	0.03		
Milos S3	78.02	0.11	12.69	0.75	0.06	0.12	0.90	3.93	3.40	0.02	Milos	Kutterolf et al. (2021)
2s.d.	0.50	0.05	0.33	0.09	0.07	0.04	0.06	0.34	0.23	0.04		
Milos S5	77.91	0.07	12.44	0.57	0.07	0.05	0.63	3.37	4.88	0.01	Milos	Kutterolf et al. (2021)
2s.d.	0.41	0.04	0.25	0.18	0.08	0.05	0.13	0.54	0.64	0.03		
Milos S6	77.84	0.07	12.44	0.60	0.10	0.05	0.63	3.44	4.82	0.01	Milos	Kutterolf et al. (2021)
2s.d.	0.35	0.04	0.22	0.15	0.08	0.04	0.06	0.30	0.18	0.03		
Milos S10	77.93	0.05	12.48	0.59	0.09	0.04	0.62	3.40	4.79	0.01	Milos	Kutterolf et al. (2021)
2s.d.	0.31	0.04	0.22	0.13	0.07	0.03	0.04	0.21	0.12	0.02		

Table 2
A summary of averaged trace elements compositions of the MIS 5e group of tephras (this study), distal and proximal KPT (Satow et al., 2015; Kutterolf et al., 2021), Milos (Kutterolf et al., 2021) and Acıgöl (Tomlinson et al., 2015). Full geochemical data sets acquired in this study are available in the Supplementary material file.

Name	Rb	Sr	Y	Zr	Nb	Ba	La	Ce	Pr	Nd	Sm	Eu	Gd	Dy	Er	Yb	Lu	Hf	Ta	Pb	Th	U
LC31 6.37	148.5	43.0	13.8	48.3	22.8	442.7	22.3	39.0	3.6	10.7	2.1	0.2	1.7	2.1	1.4	1.7	0.3	1.9	1.9	13.2	14.8	5.8
LC21 10.345	167.0	49.9	16.6	58.8	26.6	504.5	26.9	46.1	4.2	13.3	2.3	0.2	2.1	2.4	1.7	2.1	0.3	2.4	2.3	16.4	18.2	7.2
ODP967 8.87	141.4	41.3	12.7	48.1	22.0	431.0	21.5	36.7	3.4	10.4	1.8	0.2	1.6	1.9	1.3	1.6	0.2	1.9	1.9	11.2	14.5	5.8
ODP967 7.61	146.3	41.0	14.4	51.1	23.8	446.8	23.1	39.7	3.6	11.5	2.1	0.2	1.8	2.3	1.5	1.7	0.3	2.1	2.1	12.1	16.0	6.1
Nahal Aqev	142.2	41.3	13.5	47.3	22.6	437.0	21.8	37.4	3.7	10.5	1.9	0.2	1.6	1.9	1.4	1.4	0.2	1.9	1.9	11.0	15.0	5.9
KPT-frothy	184.0	46.0	14.8	54.4	28.3	515.6	24.8	47.2	4.1	12.1	2.5	0.2	2.0	1.9	1.5	1.9	0.3	2.1	2.3	15.4	17.4	7.7
KPT (POS cores)	161.3	42.2	13.5	48.1	25.0	440.6	22.3	42.8	3.8	11.2	2.1	0.2	1.8	2.1	1.4	1.6	0.3	1.9	2.1	15.1	15.7	7.1
KPT (POS cores)	146.1	43.6	14.5	51.2	23.2	455.5	24.1	41.9	3.8	11.6	2.0	0.2	2.0	2.1	1.5	1.8	0.3	2.1	2.2	13.0	16.3	6.1
KPT (POS cores)	174.4	47.7	15.1	52.4	26.7	518.8	25.2	46.2	4.1	12.3	2.1	0.3	1.9	2.3	1.5	2.0	0.3	2.1	2.3	15.8	17.2	7.2
LC21 KPT	149.7	42.0	13.5	50.1	23.6	443.0	22.5	39.3	3.5	11.0	2.1	0.2	1.8	2.1	1.4	1.7	0.3	< LOD	2.1	14.3	14.9	6.0
LC21 9.935	186.8	54.1	17.4	64.8	28.9	602.9	30.0	49.4	4.7	14.2	3.0	0.3	2.5	2.6	1.7	2.4	0.4	2.7	2.6	14.6	20.6	8.1
Guneydag	266.1	0.2	31.3	66.1	32.8	2.6	12.5	28.2	3.2	12.0	3.3	0.0	3.6	4.8	3.2	3.7	0.5	< LOD	3.4	29.9	29.5	11.2
Korudag	255.3	21.5	28.7	86.4	30.5	117.8	18.5	37.6	3.9	14.1	2.7	0.1	3.0	4.3	3.0	3.5	0.5	< LOD	3.1	33.9	30.0	10.7
Milos S1	112.5	51.9	18.2	58.6	9.5	542.3	24.7	49.9	4.8	15.2	2.8	0.5	2.7	2.6	1.8	2.5	0.4	2.4	0.9	9.3	12.4	3.5
Milos S2	111.9	45.3	16.9	54.6	9.1	512.2	24.1	48.9	4.7	14.9	2.8	0.4	2.4	2.7	1.7	2.4	0.3	2.1	0.9	9.2	11.7	3.4
Milos S3	119.8	53.6	18.5	59.0	9.5	570.6	26.6	52.3	5.0	15.7	3.0	0.5	2.6	2.8	1.9	2.5	0.3	2.4	1.0	10.3	12.8	3.7
Milos S5	162.0	17.9	30.5	56.6	14.2	330.0	20.6	44.3	4.6	15.5	3.5	0.1	3.7	4.6	3.2	4.0	0.6	2.6	1.7	14.5	17.4	5.9
Milos S6	166.6	19.0	31.0	55.5	14.5	352.3	20.5	45.1	4.7	15.7	3.7	0.2	3.6	4.6	3.2	4.1	0.6	2.5	1.6	13.9	18.1	5.9

becomes much harder to disentangle these 2 tephras (See error bars on Fig. 3). Therefore, whilst the variance between the LC31 6.37 and NAQ tephra could represent the products of two separate volcanic eruptions, this cannot be demonstrated with the current data.

It is worth noting that LC21 993.5 and LC21 10.345 are indistinguishable on geochemical plots (Fig. 3b), which might imply these two tephras are generated in one eruption and the younger tephra is reworked. However, the much higher abundance of shards in LC21 993.5 compared to LC21 10.345 indicate this upward reworking process is not possible. The possibility of LC21 10.345 to be a separate eruption or a reworking deposit will be further discussed with other evidence in Section 3.5.

Comparison of the major element composition of this MIS 5e group of tephra layers and the single glass compositions of KPT proximal deposits (Kutterolf et al., 2021) and distal tephra in marine sequences (ODP967 8.870, Satow, 2012; LC21 12.465, Satow et al., 2015; KL51-510, Wulf et al., 2020; KPT from POS cores, Kutterolf et al., 2021), the proximal deposits of Acıgöl (Tomlinson et al., 2015) and Milos systems (Kutterolf et al., 2021) (Fig. 3e and f, Table 1) shows that they are very similar from one another, sharing high SiO_2 and very low CaO and FeO wt% values. Overall, although the MIS 5e group of tephras mostly overlap with the KPT, it is impossible to determine which volcano produce the eruptions solely based on major elements.

The trace element spider diagrams and binary diagrams (Fig. 3g–k) show that the MIS 5e group of tephra are indistinguishable from the KPT, but different from products of Milos and Acıgöl systems. This implies that the MIS 5e tephra layers originate from the Kos-Nisyros-Yali volcanic system and represent a previously unknown highly silicic MIS 5e eruption. It is worth noting the major elements composition of the KPT show a relatively wide compositional range. As the MIS 5e group of tephras are from the same volcanic system, it is possible that the compositions of this tephra also display a wide range which sit across the LC31 6.37 and the NAQ tephra, depending on the magmatic process which produced this MIS 5e eruption (see Section 3.5).

3.3. Age considerations of MIS 5e tephras

Both ODP967 7.610 and LC21 993.5 are found close to the highest peak of MIS 5e in their planktic foraminifera (*G. ruber*) $\delta^{18}O$ records (Fig. 2) and within the sapropel S5 layer, which is the most distinctive sapropel in the Eastern Mediterranean sapropel chronology and stratigraphy. S5 is dated to 128.3–121.5 ka according to the chronology for core LC21, which derived from a combination of multiple radiocarbon dates, imported tephra ages and tuning to the U/Th-dated Soreq Cave (Israel) speleothem $\delta^{18}O$ record (Grant et al., 2016). Satow et al. (2020) estimated an age of 126.4 ± 2 ka for tephra ODP967 7.610 by linear interpolation between the ages for the start and termination of sapropel 5. The tephra in Nahal Aqev lies in a confirmed stratigraphical context corresponding to an archaeological layer 11, which is dated to MIS 5e via luminescence techniques (pIR-IR_{250} on alkali feldspar) (Barzilai et al., 2022). The visible tephra found in core LC31, is bracketed by luminescence samples 10 cm above and below, yielding ages of 116 ± 7 and 135 ± 8 ka (pIR-IR_{225} on K-feldspar). LC31 age-depth model is based on five radiocarbon dates, fourteen luminescence dates and ages of other correlated visible tephras. Bayesian modelled age of the dataset for LC31 yields an age of 129.6 ± 6 ka for this tephra, lies within the uncertainties of estimated age of ODP967 7.610. It is, however, possible to attempt to refine the age for this tephra by combining additional information as a Bayesian phase age model (e.g. Blockley et al., 2008; Bronk Ramsey et al., 2015). In this case, an age is developed for this tephra, combining the chronological information from all four sites (start and termination dates of sapropel S5 in ODP967 and LC21, luminescence dates above and below the tephra in LC31 and Nahal Aqev) as two contiguous phases with a Boundary separating the phases designated as the eruption age. This yields, age of 124.9 ± 2 ka for the MIS5e Kos tephra (see supplementary).

Additional tephrostraitgraphic work from other sequences is required to confirm whether LC21 10.345 is a separate eruption from the Kos volcano. If further studies confirmed this eruption, the tephra was detected in the same layer with a few P-11 tephra shards, dated to 133.5 ± 2 ka by interpolating the LC21 core chronology (Satow et al., 2015).

3.4. Chronological implications

The occurrence of two Kos tephras, dated to the MIS5e and 133 ka, has significant implications for chronologies of Eastern Mediterranean sediments and palaeoenvironmental reconstructions based on them. Currently known occurrences of the MIS 5e Kos tephras are to the east of the volcano, including abundant shards in the Nahal Aqev sequence 1000 km distant, implying widespread

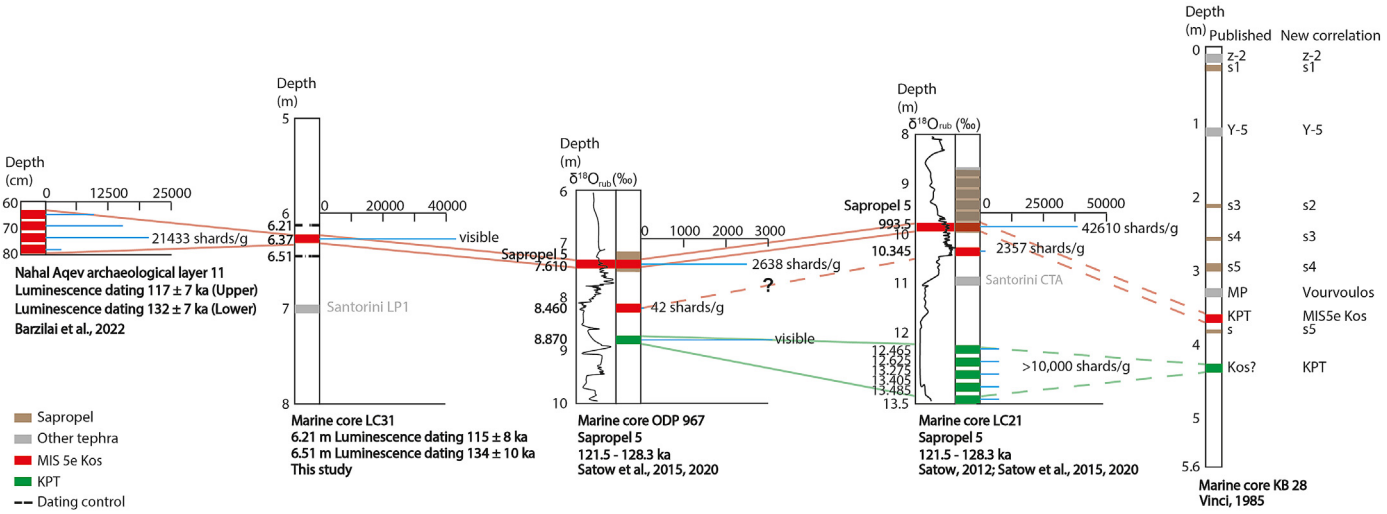

Fig. 2. Tephrostratigraphies with shard concentrations of marine cores LC31, ODP967, LC21 and NAQ. Red lines indicate correlation. Dashed red lines indicate potential correlation. Green lines indicate the correlations of KPT. Marine oxygen isotope data from: LC21 (Grant et al., 2012), ODP967 (Grant et al., 2022).

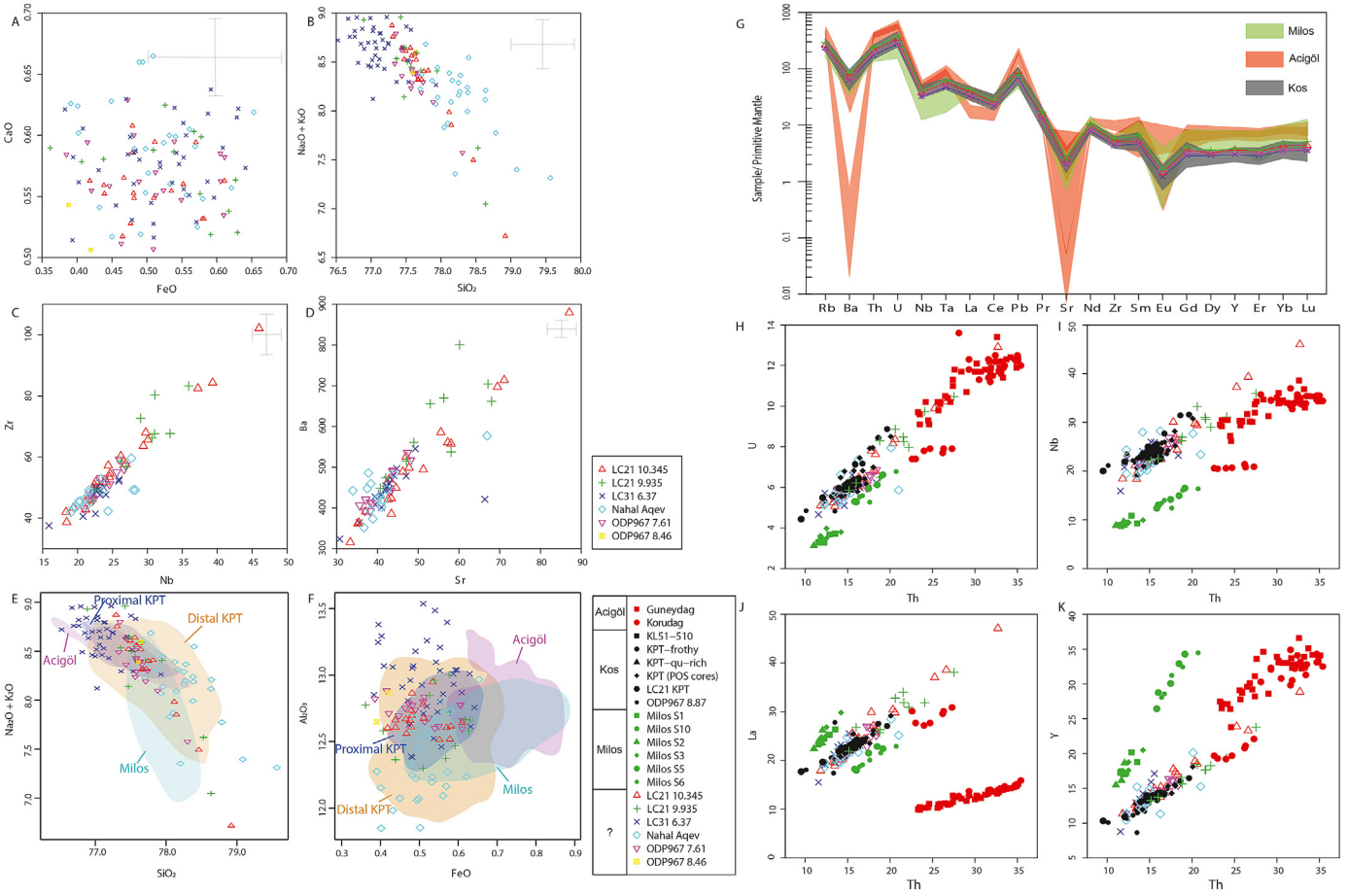

Fig. 3. Geochemical comparison between the KPT and MIS 5e tephra. A – d) Bi-plots of selected major and trace elements of the MIS 5e group of tephra (more plots see Supplementary); e – f) Comparison of major elements of the MIS 5e group of tephras to the KPT, and eruptions of Milos and Acıgöl. The source volcano data are presented as 95% kernel densities of the data with the MIS 5e samples overlain on the shaded areas (see supplementary for detailed comparisons on each eruptions); g) Spider diagrams of trace element normalised to primitive mantle of averaged MIS 5e tephra comparing different volcanic centres (all trace element data included and presented as shaded envelopes). Note two separate red areas indicate the two eruptions from Acıgöl whilst Kos and Milos compositions are continuous; h-k) binary diagrams display selected trace elements vs. Th. Acıgöl data from Tomlinson et al. (2015); Kos data from Satow (2012); Satow et al. (2015); Wulf et al. (2020); Kutterolf et al. (2021); Milos data from Kutterolf et al. (2021). Error bars represent 2 s.d. Dispersion of secondary standard measurements.

easterly dispersal of this ash (Fig. 1). Consequently, it is very likely that this layer will be found in other Eastern Mediterranean sites, greatly aiding integration of chronologies for Middle Palaeolithic sites and Eastern Mediterranean terrestrial and marine palaeoenvironmental archives (Barzilai et al., 2022).

Another implication of the newly identified tephra is for the construction of marine sediment chronologies using sapropels. Sapropel ages are established based on tuning cyclic sedimentary cyclic features of long sequences to astronomical insolation cycles (Lourens, 2004; Grant et al., 2017). However, the identification of individual sapropels is problematic as spatial and temporal basin dynamics lead to "missing" and/or "ghost" sapropels (Cramp and O'Sullivan, 1999; Emeis et al., 2000). In previous studies tephra identified as the KPT were used to identify adjacent sapropels. The identification of new MIS5e Kos tephra, with major element geochemistry indistinguishable from that of the KPT, implies that some sapropel age attributions based on the presence of KPT-like tephra may be erroneous. Furthermore, some Eastern Mediterranean tephra are dated by estimating the sedimentation rate between identified sapropels (Druitt et al., 1999; Satow et al., 2015; Wulf et al., 2020), meaning that there is scope for misidentified sapropels to cascade additional errors.

Although there are numerous marine tephra studies in the Eastern Mediterranean, most focus on visible tephra layers (e.g., Vinci, 1985; Kutterolf et al., 2021), and it is likely that the MIS 5e Kos tephras have been undetected in most cores, since cryptotephra are not routinely examined. The existence of two Kos-like tephra layers was reported by Vinci (1985), who noted that in marine core KB28, two visible layers with Kos chemistry were stratigraphically separated by a sapropel, eliminating the possibility that they represented reworking of a single deposit. Vinci (1985) identified the sapropel above the upper Kos tephra as sapropel 5, based correlation of W-2 tephra to the Santorini Middle Pumice, whilst the sapropel between the two Kos tephra was assigned to sapropel 6 (Fig. 2). However, both Vourvoulos (dated to 126.5 ± 2.9 ka) tephra and Santorini Middle Pumice (dated to 121.8 ± 2.9 ka) were originated from the Santorini volcano and having similar major elements compositions, which have been detected in serval marine sediment sequences (Satow et al., 2015; Wulf et al., 2020). Mean glass microprobe composition data of KB28 W-2 from Vinci (1985) was compared to both Middle Pumice and Vourvoulos, showing no evidence for a robust correlation to the Santorini Middle Pumice over Vourvoulos (see supplementary). The sapropels identified as sapropel S5 and S6 by Vinci (1985) could therefore be sapropels S4 and S5, an attribution which is consistent with our new findings. However, the detected Vourvoulos is found stratigraphically within the sapropel S5 in LC21, with Middle Pumice (W-2 tephra) detected below the S5 and above the KPT, which might challenge our tentative correlations. In either circumstance, two Kos tephras in the core KB28 further highlight the complexities of Kos eruptions and such chemistry cannot be taken for granted to correlate to the KPT.

The younger Kos eruptions are the first tephras identified in the Eastern Mediterranean sequence that could be used as a marker for the onset of MIS 5e. The detection of the first widespread tephras at this age, along with the sapropel 5 close to it stratigraphically, is an advance for the construction of an Eastern Mediterranean chronological framework. Overall, this paper highlights the importance of examining cryptotephra in the Eastern Mediterranean and the necessity of performing trace element analysis routinely for tephra identification. It is now no longer possible to attribute a tephra to the KPT based on major element chemistry and sapropel stratigraphy alone.

3.5. Volcanological implications

Although we have established at least two Kos eruption events in MIS 5e, ~30-40 k year younger than the KPT, there is no proximal evidence for these younger eruptions. This could be because: 1) The younger Kos tephra may s have not generated a proximal pyroclastic flow or lapilli/ash on land if this has been effectively been transported distally to the volcano by the magnitude of the eruption; 2) The proximal units have been, misidentified as reworked products of the KPT, since the two eruptions are chemically almost indistinguishable; 3) They have been eroded by later eruptions; or 4) the MIS 5e eruption could be phreatic, with subaqueous products yielding few terrestrial outcrops. Recently two Nisyros eruptions have been identified, which only appear to have been recorded in marine sequences (Kutterolf et al., 2021). Moreover, some radiometric dates on the KPT were performed on the basal ash and pumice flow (Smith et al., 1996) and others do not report exact sampling locations (Smith et al., 2000; Bachmann et al., 2010a), leading to some ambiguity. Moreover, as the Kos volcano is on a subduction-related silicic volcanic centre, it might be worth applying the new high precision (U–Th)/He dating techniques (Danišík et al., 2017) on the zircon of KPT deposits, to compare with the results of current existing Ar/Ar and U–Pb dating results on the KPT (Smith et al., 1996, 2000; Bachmann et al., 2010a; Guillong et al., 2014).

The eruption vent of the MIS 5e Kos eruptions remains unclear. However, Piper and Pe-Piper (2020) have reported pumiceous tuffites of the Agios Stylianos and Giapili reservoir outcrops on a raised MIS5e terrace in eastern Kos. Based on the lithological evidence and stratification, Piper and Pe-Piper (2020) identified these outcrops as reworked KPT. However, the variance of composition and grain sizes of these outcrops are different from the main KPT sections in central Kos (Allen et al., 1999). Furthermore, the outcrops occur in eastern Kos, which also matches the possible main plume direction of the MIS 5e Kos eruptions, implying that they may actually represent proximal deposits of the MIS 5e Kos eruptions. Lastly, Piper and Pe-Piper (2020) were unaware of MIS 5e Kos eruptions, and hence were limited to differentiating between the KPT and Kefalos eruption, adding to the scope for misidentification of theirs when correlating their pumiceous tuffites. Future radiometric dating of these and other proximal outcrops attributed to the KPT eruption should clarify their provenance.

Due to the evolved nature and size of the MIS 5e Kos tephra, we propose that it is most likely a single eruption across all sites (i.e. NAQ tephra, LC31 6.37, LC21 993.5, ODP967 7.610). ODP967 8.460 is tentatively correlated to LC21 10.345 with the possibility of representing another Kos eruption, based on their stratigraphic positions between the KPT and the MIS5e Kos tephra, identical geochemical compositions, and the low quantity of shards. However, due to low abundance of shards number and the stratigraphic proximity between two layers, ODP967 8.460 was also suggested to be a possible reworking/contamination of the primary deposit of ODP967 8.870 (correlated to the KPT) (Satow, 2012). LC21 10.345 is also possibly a reworked layer of LC21 993.5 caused by downwards bioturbation or remobilisation of sediments of either LC21 993.5 or LC21 12.465 by turbidite flows (e.g. Koutrouli et al., 2018). However, the shards counting profile of LC21 shows it to be a distinct layer with no background tephra between it and other two tephras with similar chemistry (Fig. 2; Satow et al., 2015). The low abundance of shards could be explained by the location of core LC21 proximal to the Kos and a low amount of ashes dispersed during the eruption. Additionally, the deposition of tephra is related to a large number of factors in the marine environments (Freundt et al., 2023), where the absence of LC21 10.345 and ODP967 8.460 in the limited existing regional crypto-tephrostratigraphies does not mean these

tephras would not be detected in future work. Consequently LC21 10.345 (with the possibility of correlating to ODP967 8.460) probably represents another eruption from Kos. Currently, this conclusion is limited by the fact that LC21 10.345 is only found in one sequence and the low chances that Kos volcano was triggered twice and produced highly silicic eruptions during a relatively short period of time (~9 ka). However, the current evidence does preclude the possibility of multiple Kos eruptions during MIS5e. Additional tephrostratigraphic work is needed to test this hypothesis. Moreover, the Kos-Nisyros-Yali volcanic complex has generated many eruptions from the same magma reservoirs (Dietrich and Lagios, 2018). The system goes through a period of maturation, fermentation and recovery, resulting in the evolved magma composition (de Maisonneuve et al., 2021). Such a cyclic system could repeatedly generate magma of the same or very similar composition from basaltic andesite to high-SiO_2 rhyolite (Bachmann et al., 2010b). Because only the KPT was identified at the end of the cycle at 161 ka, it was believed that this eruption emptied the magma chamber and the post-caldera magma system became more mafic and drier again (Bachmann and Huber, 2016; Bachmann et al., 2019). However, unlike the rhyodacitic to rhyolitic products of younger magmatic evolution cycles (Yali and Nisyros), the MIS 5e Kos tephras are almost indistinguishable from the KPT. Therefore, it suggests that either: 1) the MIS 5e events and LC21 10.345 was erupted from the remnant of the KPT magma or; 2) The MIS 5e and LC21 10.345 magma evolved in a sub chamber within the KPT plumbing system and was not evacuated during the 161 ka eruption. Subsequent reactivation of the system by melt injection could have triggered an eruption, or even potentially crustal deformation due to rapid sea level rise at the start of MIS 5e, as has been suggested for other island volcanoes in the region (Satow et al., 2021). Additional work is needed to understand the Late Quaternary eruptive history of the Kos-Nisyros-Yali volcanic complex.

4. Conclusions

A new eruption dated to the start of MIS 5e (124.9 ± 2 ka) has been identified across multiple sites in the Eastern Mediterranean, and another eruption showing identical chemical compositions dated to 133.5 ± 2 ka was identified in the LC21 sequence (i.e. LC31 10.345). Trace element data indicates that both tephra/cryptotephra are originated from the Kos volcano, with almost indistinguishable major and trace element compositions to Kos Plateau Tuff (KPT). The KPT is used as a widespread chronological and stratigraphic marker for many palaeoenvironmental archives, however correlation to it are mostly based on major element compositions. This study discusses the weakness of using major element concentrations alone, as multiple tephra layers from other source volcanoes have major element geochemical fingerprints which are indistinguishable from the KPT and only trace elements are able to separate these layers. This must be considered for any other palaeoenvironmental reconstructions using tephra correlation as isochron markers in the other parts of the world, because most tephra correlations are purely based on their major element characteristics. The KPT was widely correlated in the region for palaeoenvironmental records. The detection of new major eruptions with similar chemical compositions could shift previous correlations and palaeoenvironmental interpretations based on these correlations. The new MIS 5e tephras could also present a rare opportunity for correlating palaeoenvironmental and archaeological records at the start of MIS 5e in a key region for understanding the dispersal of humans out of Africa. Based on the sedimentological evidence eliminating the possibility of reworking, a tephra dated to 133.5 ± 2 ka could represent another eruption from the Kos volcano. However, further work is required to confirm the existence of this additional eruption and secure its age and stratigraphic position.

Furthermore, the Kos-Nisyros-Yali volcanic complex is regarded as a classic example of a cycling caldera system. Our results indicate that unexpected eruptions of the Kos volcano could happen not as part of the classic eruption cycle, suggesting there is much to learn about the nature of the Kos volcanic system.

Author contribution

S.Z., S.B., S.J.A., C.S. and C.M. developed the project idea. S.Z. and S.B. analysed glass major element using EPMA. S.Z. and C.M. analysed trace element compositions using LA-ICP-MS. S.Z. and S.J.A. performed luminescence dating on core LC31. C.S., O.B., E.B., D.W., R.T. provided samples and background information of sites ODP967, LC21 and Nahal Aqev. S.Z. wrote the manuscript with contributions from all co-authors.

Declaration of competing interest

The authors declare that they have no known competing financial interests or personal relationships that could have appeared to influence the work reported in this paper.

Data availability

The data will be shared in supplementary file

Acknowledgement

The British Ocean Sediment Core Research Facility (BOSCORF) is thanked for providing sediment subsamples. The research was funded by the Leverhulme Trust (PG-2017-087 to S.B., E.A., S.J.A. and M.D.P.) and Irene Levi-Sala CARE Archaeological Foundation. SA's contribution to this work was partly supported by the Research Council of Norway, through its Centres of Excellence funding scheme, SFF Centre for Early Sapiens Behaviour (SapienCE), project number 262618. The Nahal Aqev excavation was directed by O.B. and E.B. under the funding of the Max Planck-Weizmann Centre for Integrative Archaeology and Anthropology. O.B. and E.B. wishes to thank Maya Oron (Israel Antiquities Authority) for her invaluable contribution to the Nahal Aqev excavation research. The authors also thank the editor Professor Giovanni Zanchetta as well as two anonymous reviewers for their helpful and constructive reviews and recommendations, which have greatly improved the submitted manuscript.

Appendix A. Supplementary data

Supplementary data to this article can be found online at https://doi.org/10.1016/j.quascirev.2023.108054.

References

Allen, S.R., 2001. Reconstruction of a major caldera-forming eruption from pyroclastic deposit characteristics: Kos Plateau Tuff, eastern Aegean Sea. J. Volcanol. Geoth. Res. 105, 141–162. https://doi.org/10.1016/S0377-0273(00)00222-5.

Allen, S.R., Stadlbauer, E., Keller, J., 1999. Stratigraphy of the Kos Plateau Tuff: product of a major quaternary explosive rhyolitic eruption in the eastern aegean, Greece. Int. J. Earth Sci. 88, 132–156.

Bachmann, O., Huber, C., 2016. Silicic magma reservoirs in the Earth's crust. Am. Mineral. 101, 2377–2404. https://doi.org/10.2138/am-2016-5675.

Bachmann, O., Allen, S.R., Bouvet de Maisonneuve, C., 2019. The kos–nisyros–yali volcanic field. Elements 15, 191–196. https://doi.org/10.2138/gselements.15.3.191.

Bachmann, O., Schoene, B., Schnyder, C., Spikings, R., 2010a. The 40Ar/39Ar and U/Pb dating of young rhyolites in the Kos-Nisyros volcanic complex, Eastern

Aegean Arc, Greece: age discordance due to excess 40Ar in biotite. G-cubed 11. https://doi.org/10.1029/2010GC003073.
Bachmann, O., Wallace, P.J., Bourquin, J., 2010b. The melt inclusion record from the rhyolitic Kos Plateau Tuff (Aegean Arc). Contrib. Mineral. Petrol. 159, 187–202. https://doi.org/10.1007/s00410-009-0423-4.
Barzilai, O., Oron, M., Porat, N., White, D., Timms, R., Blockley, S., Zular, A., Avni, Y., Faershtein, G., Weiner, S., Boaretto, E., 2022. Expansion of eastern Mediterranean Middle Paleolithic into the desert region in early marine isotopic stage 5. Sci. Rep. 12, 1–13. https://doi.org/10.1038/s41598-022-08296-9.
Blockley, S.P., Pyne-O'Donnell, S.D., Lowe, J.J., Matthews, I.P., Stone, A., Pollard, A.M., Turney, C.S., Molyneux, E.G., 2005. A new and less destructive laboratory procedure for the physical separation of distal glass tephra shards from sediments. Quat. Sci. Rev. 24, 1952–1960. https://doi.org/10.1016/j.quascirev.2004.12.008.
Blockley, S.P., Ramsey, C.B., Pyle, D.M., 2008. Improved age modelling and high-precision age estimates of late Quaternary tephras, for accurate palaeoclimate reconstruction. J. Volcanol. Geoth. Res. 177, 251–262. https://doi.org/10.1016/j.jvolgeores.2007.10.015.
Bouvet de Maisonneuve, C., Bachmann, O., Burgisser, A., 2009. Characterization of juvenile pyroclasts from the Kos Plateau Tuff (Aegean Arc): insights into the eruptive dynamics of a large rhyolitic eruption. Bull. Volcanol. 71, 643–658. https://doi.org/10.1007/s00445-008-0250-x.
Bronk Ramsey, C., Albert, P.G., Blockley, S.P., Hardiman, M., Housley, R.A., Lane, C.S., Lee, S., Matthews, I.P., Smith, V.C., Lowe, J.J., 2015. Improved age estimates for key Late Quaternary European tephra horizons in the RESET lattice. Quat. Sci. Rev. 118, 18–32. https://doi.org/10.1016/j.quascirev.2014.11.007.
Cramp, A., O'Sullivan, G., 1999. Neogene sapropels in the Mediterranean: a review. Mar. Geol. 153, 11–28. https://doi.org/10.1016/S0025-3227(98)00092-9.
Danišík, M., Schmitt, A.K., Stockli, D.F., Lovera, O.M., Dunkl, I., Evans, N.J., 2017. Application of combined U-Th-disequilibrium/U-Pb and (U-Th)/He zircon dating to tephrochronology. Quat. Geochronol. 40, 23–32.
de Maisonneuve, C.B., Forni, F., Bachmann, O., 2021. Magma reservoir evolution during the build up to and recovery from caldera-forming eruptions–A generalizable model? Earth Sci. Rev. 218, 103684. https://doi.org/10.1016/j.earscirev.2021.103684.
Dietrich, V.J., Lagios, E., 2018. Nisyros Volcano: The Kos-Yali-Nisyros Volcanic Field: Springer International Publishing. 339 p. https://doi.org/10.1007/978-3-319-55460-0.
Druitt, T.H., Edwards, L., Mellors, R.M., Pyle, D.M., Sparks, R.S.J., Lanphere, M., Davies, M., Barreirio, B., 1999. Santorini volcano. Geol. Soc. Mem. 19.
Dufek, J., Bergantz, G.W., 2007. Dynamics and deposits generated by the Kos Plateau Tuff eruption: controls of basal particle loss on pyroclastic flow transport. G-cubed 8. https://doi.org/10.1029/2007GC001741.
Emeis, K.C., Sakamoto, T., Wehausen, R., Brumsack, H.J., 2000. The sapropel record of the eastern mediterranean sea—results of ocean drilling program leg 160. Palaeogeogr. Palaeoclimatol. Palaeoecol. 158, 371–395. https://doi.org/10.1016/S0031-0182(00)00059-6.
Federman, A.N., Carey, S.N., 1980. Electron microprobe correlation of tephra layers from eastern Mediterranean abyssal sediments and the island of Santorini. Quat. Res. 13 (2), 160–171. https://doi.org/10.1016/0033-5894(80)90026-5.
Freundt, A., Schindlbeck-Belo, J.C., Kutterolf, S., Hopkins, J.L., 2023. Tephra layers in the marine environment: a review of properties and emplacement processes. Geol. Soc, London, Special Publications 520, SP520–SP2021. https://doi.org/10.1144/SP520-2021-50.
Grant, K.M., Amarathunga, U., Amies, J.D., Hu, P., Qian, Y., Penny, T., Rodriguez-Sanz, L., Zhao, X., Heslop, D., Liebrand, D., Hennekam, R., 2022. Organic carbon burial in Mediterranean sapropels intensified during Green Sahara Periods since 3.2 Myr ago. Commun. Earth Environ 3, 11.
Grant, K.M., Grimm, R., Mikolajewicz, U., Marino, G., Ziegler, M., Rohling, E.J., 2016. The timing of Mediterranean sapropel deposition relative to insolation, sea-level and African monsoon changes. Quat. Sci. Rev. 140, 125–141. https://doi.org/10.1016/j.quascirev.2016.03.026.
Grant, K.M., Rohling, E.J., Bar-Matthews, M., Ayalon, A., Medina-Elizalde, M., Ramsey, C.B., Satow, C., Roberts, A.P., 2012. Rapid coupling between ice volume and polar temperature over the past 150,000 years. Nature 491, 744–747.
Grant, K.M., Rohling, E.J., Westerhold, T., Zabel, M., Heslop, D., Konijnendijk, T., Lourens, L., 2017. A 3 million year index for North African humidity/aridity and the implication of potential pan-African Humid periods. Quat. Sci. Rev. 171, 100–118. https://doi.org/10.1016/j.quascirev.2017.07.005.
Guillong, M.V., von Quadt, A., Sakata, S., Peytcheva, I., Bachmann, O., 2014. LA-ICP-MS Pb–U dating of young zircons from the Kos–Nisyros volcanic centre. SE Aegean arc. J. Anal. At. Spectrom. 29, 963–970. https://doi.org/10.1039/c4ja00009a.
Hardiman, J.C., 1999. Deep sea tephra from Nisyros island, eastern Aegean Sea, Greece. Geol. Soc. Spec. Publ. 161 (1), 69–88. https://doi.org/10.1144/GSL.SP.1999.161.01.06.
Koutrouli, A., Anastasakis, G., Kontakiotis, G., Ballengee, S., Kuehn, S., Pe-Piper, G., Piper, D.J.W., 2018. The early to mid-Holocene marine tephrostratigraphic record in the Nisyros-Yali-Kos volcanic center, SE Aegean Sea. J. Volcanol. Geoth. Res. 366, 96–111. https://doi.org/10.1016/j.jvolgeores.2018.10.004.
Kutterolf, S., Freundt, A., Druitt, T.H., Mcphie, J., Nomikou, P., Pank, K., Schindlbeck-Belo, J.C., Hansteen, T.H., Allen, S.R., 2021. The medial offshore record of explosive volcanism along the central to eastern Aegean Volcanic Arc: 1. Tephra ages and volumes, eruption magnitudes and marine sedimentation rate variations. G-cubed 22. https://doi.org/10.1029/2021GC010010, 2021GC010010.
Lourens, L.J., 2004. Revised tuning of ocean drilling program site 964 and KC01B (mediterranean) and implications for the δ18O, tephra, calcareous nannofossil. and geomagnetic reversal chronologies of the past 1.1 Myr. Paleoceanography. 19 (PA3010). https://doi.org/10.1029/2003PA000997.
Margari, V., Pyle, D.M., Bryant, C., Gibbard, P.L., 2007. Mediterranean tephra stratigraphy revisited: results from a long terrestrial sequence on Lesvos Island, Greece. J. Volcanol. Geoth. Res. 163 (1–4), 34–54. https://doi.org/10.1016/j.jvolgeores.2007.02.002.
Piper, D.J., Pe-Piper, G., 2020. A reworked isolated deposit of the Kos Plateau Tuff and its significance for dating raised marine terraces, Kos, Greece. Geol. Mag. 157, 2021–2032. https://doi.org/10.1017/S0016756820000254.
Satow, C., Grant, K.M., Wulf, S., Schulz, H., Mallon, A., Matthews, I., Lowe, J., 2020. Detection and characterisation of eemian marine tephra layers within the sapropel s5 sediments of the aegean and levantine seas. Quaternary 3, 6. https://doi.org/10.3390/quat3010006.
Satow, C., Gudmundsson, A., Gertisser, R., Ramsey, C.B., Bazargan, M., Pyle, D.M., Wulf, S., Miles, A.J., Hardiman, M., 2021. Eruptive activity of the Santorini Volcano controlled by sea-level rise and fall. Nat. Geosci. 14, 586–592. https://doi.org/10.1038/s41561-021-00783-4.
Satow, C., Tomlinson, E.L., Grant, K.M., Albert, P.G., Smith, V.C., Manning, C.J., Ottolini, L., Wulf, S., Rohling, E.J., Lowe, J.J., Blockley, S.P.E., 2015. A new contribution to the late quaternary tephrostratigraphy of the mediterranean: aegean sea core LC21. Quat. Sci. Rev. 117, 96–112. https://doi.org/10.1016/j.quascirev.2015.04.005.
Satow, C.G., 2012. The Tephrostratigraphy of Three, Late Quaternary, Mediterranean Marine Cores [Ph.D. Thesis]. University of London, pp. 244–258.
Smith, P.E., Evensen, N.M., York, D., 2000. Under the volcano: a new dimension in Ar-Ar dating of volcanic ash. Geophys. Res. Lett. 27, 585–588. https://doi.org/10.1029/1999GL008451.
Smith, P.E., York, D., Chen, Y., Evensen, N.M., 1996. Single crystal 40Ar-39Ar dating of a Late Quaternary paroxysm on Kos, Greece: concordance of terrestrial and marine ages. Geophys. Res. Lett. 23, 3047–3050. https://doi.org/10.1029/96GL02759.
Tomlinson, E.L., Smith, V.C., Albert, P.G., Aydar, E., Civetta, L., Cioni, R., Çubukçu, E., Gertisser, R., Isaia, R., Menzies, M.A., Orsi, G., 2015. The major and trace element glass compositions of the productive Mediterranean volcanic sources: tools for correlating distal tephra layers in and around Europe. Quat. Sci. Rev. 118, 48–66. https://doi.org/10.1016/j.quascirev.2014.10.028.
Vinci, A., 1985. Distribution and chemical composition of tephra layers from Eastern Mediterranean abyssal sediments. Mar. Geol. 64, 143–155.
Wegwerth, A., Dellwig, O., Wulf, S., Plessen, B., Kleinhanns, I.C., Nowaczyk, N.R., Jiabo, L., Arz, H.W., 2019. Major hydrological shifts in the Black Sea "Lake" in response to ice sheet collapses during MIS 6 (130–184 ka BP). Quat. Sci. Rev. 219, 126–144. https://doi.org/10.1016/j.quascirev.2019.07.008.
Wulf, S., Çağatay, M.N., Appelt, O., Eriş, K.K., Henry, P., 2021. Defining the Upper Nisyros Pumice (57.1±1.5 ka) as new tephra isochrone for linking early MIS-3 palaeoenvironmental records in the Aegean-Black Sea gateway: new evidence from the Sea of Marmara. Quat. Sci. Rev. 274, 107285. https://doi.org/10.1016/j.quascirev.2021.107285.
Wulf, S., Keller, J., Satow, C., Gertisser, R., Kraml, M., Grant, K.M., Appelt, O., Vakhrameeva, P., Koutsodendris, A., Hardiman, M., Schulz, H., 2020. Advancing Santorini's tephrostratigraphy: new glass geochemical data and improved marine-terrestrial tephra correlations for the past~ 360 kyrs. Earth Sci. Rev. 200, 102964. https://doi.org/10.1016/j.earscirev.2019.102964.